AIP Advances

Anisotropy engineering using exchange bias on antidot templates

F. J. T. Goncalves, R. D. Desautels, S. Su, T. Drysdale, J. van Lierop, K.-W. Lin, D. S. Schmool, and R. L. Stamps

Citation: AIP Advances **5**, 067101 (2015); doi: 10.1063/1.4922055
View online: http://dx.doi.org/10.1063/1.4922055
View Table of Contents: http://scitation.aip.org/content/aip/journal/adva/5/6?ver=pdfcov
Published by the AIP Publishing

Anisotropy engineering using exchange bias on antidot templates

F. J. T. Goncalves,[1,a] R. D. Desautels,[2] S. Su,[3] T. Drysdale,[4] J. van Lierop,[2] K.-W. Lin,[3] D. S. Schmool,[5] and R. L. Stamps[1]
[1]*SUPA, School of Physics and Astronomy, University of Glasgow, Glasgow G12 8QQ, UK*
[2]*Department of Physics and Astronomy, University of Manitoba, Winnipeg, R3T 2N2, Canada*
[3]*Department of Materials Science and Engineering, National Chung Hsing University, Taichung 402, Taiwan*
[4]*Department of Engineering, University of Glasgow, Glasgow G12 8QQ, UK*
[5]*Lab. PROMES CNRS (UPR8521), Université de Perpignan Via Domitia, 66100 Perpignan, France*

(Received 20 February 2015; accepted 18 May 2015; published online 1 June 2015)

We explore an emerging device concept based on exchange bias used in conjunction with an antidot geometry to fine tune ferromagnetic resonances. Planar cavity ferromagnetic resonance is used to study the microwave response of NiO/NiFe bilayers with antidot structuring. A large frequency asymmetry with respect to an applied magnetic field is found across a broad field range whose underlying cause is linked to the distribution of magnetic poles at the antidot surfaces. This distribution is found to be particularly sensitive to the effects of exchange bias, and robust in regards to the quality of the antidot geometry. The template based antidot geometry we study offers advantages for practical device construction, and we show that it is suitable for broadband absorption and filtering applications, allowing tunable anisotropies via interface engineering. [http://dx.doi.org/10.1063/1.4922055]

Periodic arrangements of non-magnetic holes (antidots) embedded in a continuous film are of great interest for high frequency applications due to the versatility with which microwave properties can be tailored. One can, for example, confine and direct the propagation of spin waves[1–4] for applications such as spin wave logic and interferometry.[5,6] Antidots have proven to be extremely effective in terms of modulating local effective anisotropies and coercivities by altering hole diameter and periodicity.[7–13] We show here that anisotropies in template based antidots can be modified to allow an asymmetric broadband absorption, whose frequency range is dependent on the direction of an applied field.

Unidirectional anisotropy can be introduced into a ferromagnet through exchange coupling with an antiferromagnet. This effect, called exchange bias, is often described by an effective field which causes a shift in the hysteresis loop of the ferromagnetic film, as well an increase in the coercivity.[14,15] The induced anisotropy in exchange biased antidots has been studied as a function of lattice geometry[16–20] and the interplay between internal fields.[21–23] Patterning allows tailoring of the magnitude and direction of the bias field.[24,25] Some interesting applications are within reach, by making use of multi-state remanent processes occuring in structures with combined positive and negative bias fields.[26]

Most important for the present work, the effective bias field can modify ferromagnetic resonance response.[27] Ferromagnetic resonance frequencies can be shifted upwards or downwards, depending on the strength and polarity of the bias field. In this paper, we demonstrate the existence of a unidirectional bias induced asymmetric microwave response, which we link to an unbalanced distribution of the demagnetising fields around the holes of the antidot structure.

[a]Electronic mail: fisica.francisco@gmail.com

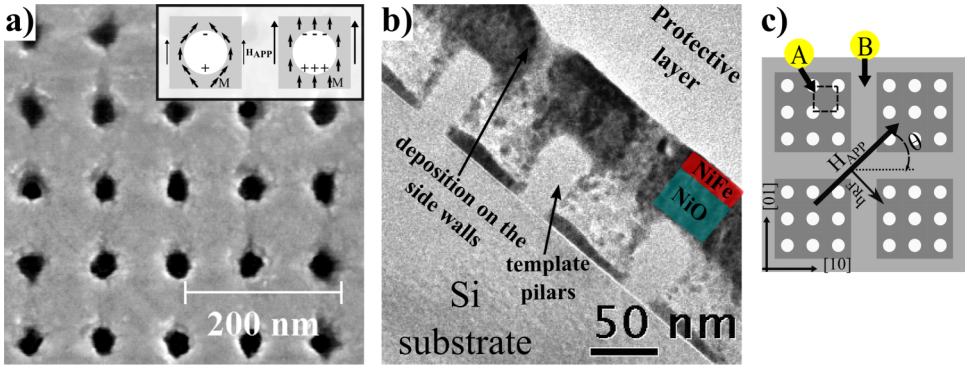

FIG. 1. a) Scanning electron microscopy image of the NiO/NiFe under investigation: NiO(36nm)/NiFe(12nm) pitch: ~100 nm, holes: 45/50 nm b) Bright field transmission electron microscopy image of the x-section and c) Schematic of the NiO/NiFe geometry and respective angle nomenclature: θ corresponds to the angle between H_{app} and lattice edges; direction [10] collinear with $\theta = 0^o$ and direction [01] collinear with $\theta = 90^o$.

In figure 1(a) we show a scanning electron microscopy(SEM) image of an antidot lattice comprising a bilayer of NiO and NiFe deposited on a template. The existing holes create a non-uniform distribution of demagnetising fields arising from local deformations in the spin configurations, as illustrated in the inset of figure 1(a).

The NiO/NiFe bilayer exhibits a room temperature exchange bias field of -1.5 mT, as shown by the lateral field displacement of the hysteresis loop in figure 2(a). What is particularly interesting is that the ferromagnetic resonance profile is highly asymmetric around zero applied field. Even for

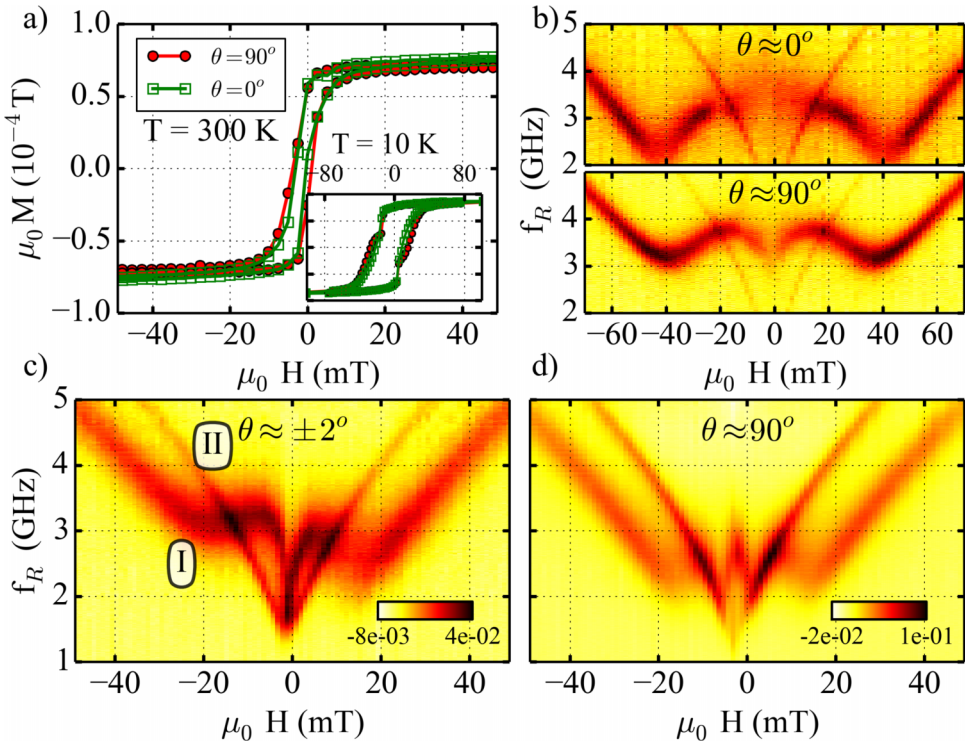

FIG. 2. The hysteresis loops in a) correspond to the NiO(36nm)/NiFe(12nm) antidot sample at the temperatures 300 K and 10 K (inset). b) The spectra corresponds to the ferromagnetic resonance spectra of NiFe(18nm) antidots taken with $\mu_0 H$ (H_{APP}) applied along $\theta = 0^o$(top) and 90^o(bottom). In this sample we do not observe asymmetric response as the system is not exchange biased. Ferromagnetic resonance spectra of the NiO/NiFe antidots taken with the applied field at: c) $\theta = \pm 2$ degrees off the lattice direction [10] and d) $\theta = 90$ degrees, collinear with the direction [01].

the small exchange bias observed here, the resonance frequency is different for a positive field, $+H_0$ (18 mT), and a negative field, $-H_0$. This is seen in figure 2(c), for a ferromagnetic resonance spectra acquired with the applied field along a direction parallel to the lattice edge. We will show that the asymmetry in the dynamics spectra provides a quantitative measure of the extent to which the pole distribution at the holes is pinned by the exchange bias.

The NiO/NiFe bilayer was deposited at room temperature and zero field using a dual ion-beam deposition system.[28] In this setup, a Kaufman ion source was used to focus an argon ion beam onto a $Ni_{80}Fe_{20}$ (at.%) and Ni targets, while an End-Hall ion source was used to bombard the substrate during the deposition of the bottom NiO layer. A fixed voltage of 140 V, at the End-Hall ion source, ensured a constant ion-beam bombardment energy. During deposition, the Ar/O_2 ratio in the End-Hall source was kept at 16% to ensure the formation of NiO. The substrate consisted of a silicon template in which the holes, with elliptical shape(45/50 nm), are periodically spaced by 100 nm.

The figure 1(b) shows a bright field transmission electron microscopy image of the antidot cross-section, cut by focused ion beam. We note that some material was sputtered onto the walls and to the bottom of the holes of the template. The thickness of the NiFe film in the bottom of the holes is negligible, but one must account for the material deposited on the curved edges of the side walls as this will add roughness to the edges of the antidots. Nevertheless this sample is, to a good approximation, an antidot array from which one should expect a ferromagnetic resonance broadened by edge roughness. Also, as illustrated in figure 1(c), the sample consists of 600 μm large arrays of holes spaced by 100 μm wide regions of continuous film. These antidot arrays and the continuous film regions are labelled as A and B, respectively. The magnetometry data shown in figure 2(a) were obtained with a Quantum Design SQUID MPMS XL-5 from 5 K to 350 K within a field range of ±2 T after initially field cooling the sample in a 2 T field from 400 K. The hysteresis loop acquired at 300 K exhibits a small exchange bias field and a rather uniform reversal process. The inset loop, acquired at 10 K, shows a stepped magnetisation curve which we attribute to reversals of the antidot region and continuous film region at different applied fields. As expected, in the low temperature regime, both coercivity and exchange bias field are enhanced.

Broadband ferromagnetic resonance spectroscopy was performed using a vector network analyser (VNA). We obtained good sensitivity by using a loop shaped micro-cavity operated in a single-port configuration. The microwave field, h_{RF}, is orthogonal to the direction of the static field, H_{APP}, applied in the plane of the sample. Each measurement begins well above the saturation field, at H_{REF} = 150 mT, where a reference spectra is acquired for background correction purposes. Then, starting at a maximum applied field H_{APP} = 60 mT, the VNA signal is swept five times and averaged; the static field is linearly reduced once the frequency sweep is completed. This procedure is repeated over the range H_{APP} = ±60 mT. Example results are shown in figures 2(b) (±80 mT), 2(c) and 2(d).

The ferromagnetic resonance data shown in figure 2(b) corresponds to a single layer of NiFe antidots, which shows no asymmetric behaviour as the exchange bias field is zero. One should note the difference in effective anisotropy, H_K^{eff}, by comparing frequencies at $\theta = 0^o$ (top) to those at $\theta = 90^o$ (bottom), as the resonance frequency $f_R(\theta = 0^o) = 2.3$ GHz is lower than $f_R(\theta = 90^o) = 3.1$ GHz for $\mu_0 H \sim 40$ mT. We attribute this change in effective anisotropy to a 5% deviation from square of the antidot lattice, observed in the figure 1(a).

Figures 2(c) and 2(d) correspond to frequency versus $\mu_0 H$ traces of the NiO/NiFe sample measured relative to the main axes of the antidot lattice, with $\theta = \pm 2^o$ and $\theta = 90^o$. In figure 2(c), a clear asymmetry is visible, with a frequency difference of approximately 0.5 GHz between $f_R(\mu_0 H = 18$ mT) and $f_R(\mu_0 H = -18$ mT).

The antidot lattice and the frame generate distinct ferromagnetic resonance spectra, denoted as resonance mode I and mode II in figure 2(c), thereby providing a useful comparison. We show later how these can be associated with the regions A and B, respectively, in figure 1(b). Both resonance modes I and II are centered at $\mu_0 H$=-1.5 mT, which we attribute to the exchange bias field. Given the distribution of the internal fields within the antidots, the resulting magnetic properties are primarily seen as an effective fourfold anisotropy in which the hard axes are along the edges [10] and [01], and the easy axes along the diagonal [11], of the unit cell. This is consistent with results of

Adeyeye et al.[16] and Wang et al.[17] In ferromagnetic resonance, the magnetic hard axis is obtained for a direction along which the resonance frequency reaches a local minimum of $f_R^{min} = 2.5$ GHz (softening) when the applied field $\mu_0 H = \pm$ 18 mT $\sim H_K^{eff}$. Mode II results from the continuous film (B) region which surrounds the antidot arrays and shows no angular dependence. By comparing the spectra of figures 2(c) and 2(d) we note a marked decrease in the frequency asymmetry from $\theta = \pm 2^o$ to $\theta = 90^o$. From observing the angular variation of the ferromagnetic resonance as a function of applied field angle, we see that the amplitude of the asymmetry drops to zero when $\theta = 0^o$ and $\theta = 90^o$. This behaviour results from competition between the fourfold anisotropy and the bias field. At $\theta = 0^0$ and 90^o, the fourfold anisotropy field is much larger than the bias field and therefore the asymmetry is less pronounced. A large asymmetry is obtained only when the applied field is off the high symmetry directions by a few degrees, with respect to the antidot lattice. The angular variation of the antidot modes in general is discussed elsewhere[29] for a different system.

In order to understand the dipolar effects on the ferromagnetic resonance, we performed finite difference micromagnetic simulations using Mumax[30] for: a 9x9 array of 35 nm circular holes spaced by 65 nm, and a continuous film region, both with identical parameters (mesh = 3.125 nm, $M_S = 820 \times 10^3$ A/m, $A_{EX} = 13 \times 10^{-12}$J/m, $\gamma = 0.02$). The resulting spectra are shown in figure 3, where we overlay the simulation results and experimental data. In the simulations, the applied field and the initial magnetic state are at an angle of 2^o from the lattice direction [10] in order to avoid artifacts at high symmetry directions.[2] The dynamics spectra were obtained by performing a Fourier transform of the time (t) dependent magnetisation, after applying a pulse in the form of $A_0 sin(t - t_0)/(2\pi t)$, where $A_0 = 1$ mT and $t_0 = 3$ ns, in the out-of plane direction. To simulate the bias field we defined a pinning field of -3 mT along the direction [11] of the antidot lattice. In the simulations, the resonance modes I and II were acquired from the magnetisation dynamics of the antidots, labelled as region A, and the continuous film, labelled as region B.

The spectra from region A resembles the asymmetric mode labelled as mode I in the experiments. At positive $\mu_0 H$ the resonance frequency, f_R^{min}, at around the H_K^{eff} is shifted downwards

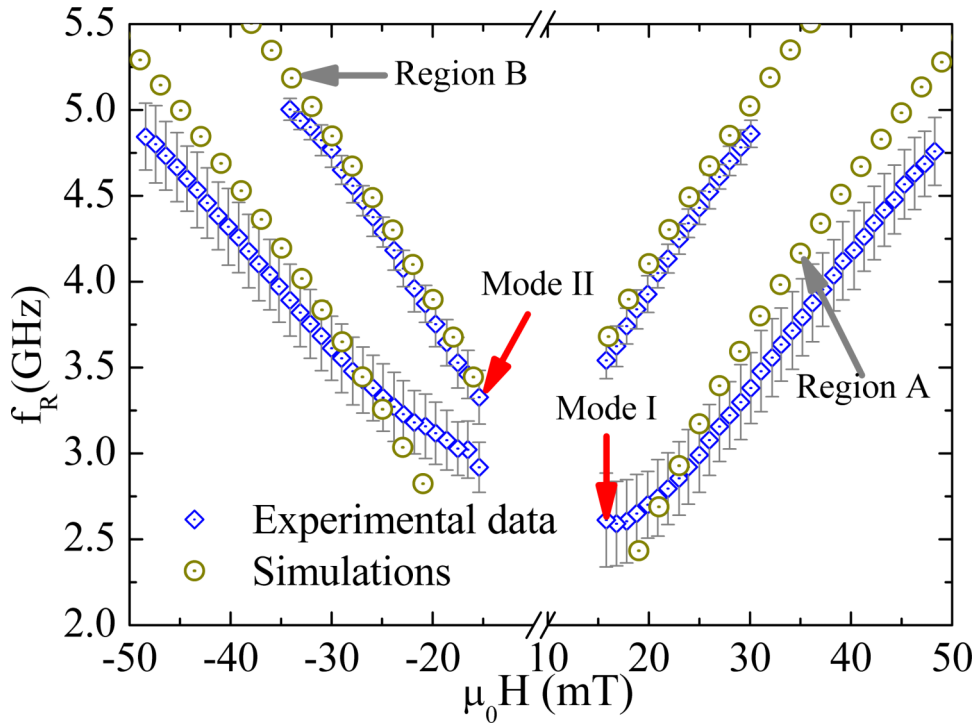

FIG. 3. Simulation results overlaid with experimental data. The simulated spectra relative to region I and region II was obtained by calculating the dynamics spectra from the antidot region (A) and the continuous film region (B) as shown in figure 1(b).

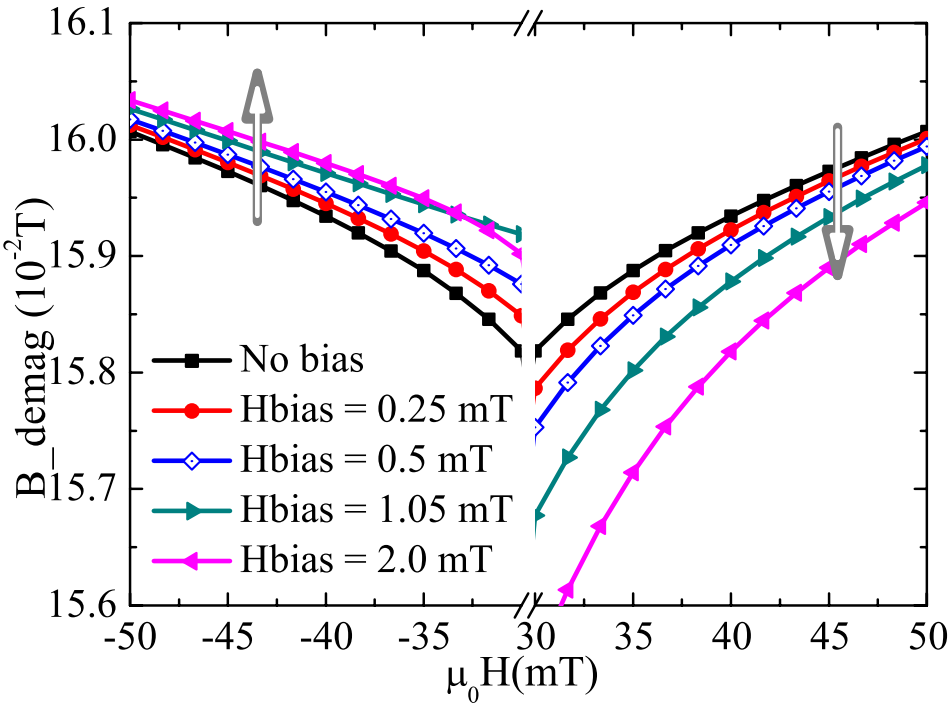

FIG. 4. Amplitude of the demagnetising field as function of $\mu_0 H$ for different H_{bias} amplitudes. The demagnetising fields where calculated by averaging over the holes set in the Mumax geometry. This field quantity measures the strength of the poles around the edges of the holes. Note the break in the $\mu_0 H$ axis. The unsaturated region ($\lesssim H_K^{eff}$) is discarded as it requires a different model of interpretation, hence the break in the field axis.

whereas at $-H_K^{eff}$ the f_R^{min} is shifted upwards. To interpret this observation we consider the effect of exchange bias in the local distribution of the poles around the holes defining the antidot geometry. Our interpretation is that the demagnetising fields are influenced by the unidirectional field acting on the magnetisation and leading to asymmetries in the ferromagnetic resonance spectra in the positive and negative directions. By sampling in region B we obtained the spectra in which the dominant resonance resembles mode II from the experimental data.

In figure 4, we show the variation of the magnitude of the demagnetising fields, B_{demag}, calculated by averaging inside the holes, as function of the applied field. Each curve corresponds to a sightly increased pinning (bias) field. For the case where the pinning field is zero, we obtain a symmetric response. When the pinning field is non-zero, we note that at positive $+\mu_0 H$ the B_{demag} decreases as the amplitude of the pinning increases. However, for $-\mu_0 H$ the behaviour has reversed, i.e. B_{demag} increases as the pinning field increases. This asymmetry in the variation of B_{demag} shows the effect of the bias field on the antidot lattice. The strength of the fields in the holes is proportional to the surface pole distribution. This indicates that the bias is affecting the ferromagnetic resonance primarily through the pole distribution.

In summary, the asymmetric response measured with ferromagnetic resonance depends on the distribution of surface magnetic poles created at the inner surfaces of the antidots. From the analysis of the demagnetising field predicted to arise from the surface pole distribution, we have shown that exchange bias can lead to large changes in the pole distribution through modifications of the magnetic order near the antidots. Most importantly, we show that the asymmetry can be created in antidots produced using a template method, which may allow a practical method for device integration.

We note that the large linewidths do not allow resolution of the finer structure, but indicate a strong dependence on the orientation of the applied field relative to both the exchange bias and antidot lattice. Because the asymmetry is driven by the exchange bias, an estimate of the operating

range in terms of temperature, would be given by the ordering temperature of the antiferromagnetic material(below 500 K for NiO). In the low temperature regime, the exchange bias is enhanced so one can expect an increase in the asymmetry. However, from the device perspective it may not be realistic to consider temperatures below 280 K.

ACKNOWLEDGEMENTS

This work was supported by Royal Society, under the Grant Ref. IE121187 and by EPSRC, under the Grants Ref. EP/L002922/1 and M024423/1. The authors would also like to acknowledge the support from EPSRC Bridging the Gap Grant, NSERC and CFI.

[1] Sebastian Neusser, Bernhard Botters, and Dirk Grundler, "Localization, confinement, and field-controlled propagation of spin waves in Ni80Fe20 antidot lattices," Physical Review B **78**(5), 054406 (2008).
[2] Silvia Tacchi, Marco Madami, Gianluca Gubbiotti, Giovanni Carlotti, Adekunle O. Adeyeye, Sebastian Neusser, Bernhard Botters, and Dirk Grundler, "Magnetic normal modes in squared antidot array with circular holes: A combined brillouin light scattering and broadband ferromagnetic resonance study," IEEE Transactions on Magnetics **46**, 172–178 (2010).
[3] C.-L. Hu, R. Magaraggia, H.-Y. Yuan, C. S. Chang, M. Kostylev, D. Tripathy, A. O. Adeyeye, and R. L. Stamps, "Field tunable localization of spin waves in antidot arrays," Applied Physics Letters **98**(26), 262508 (2011).
[4] J. Sklenar, V. S. Bhat, L. E. DeLong, O. Heinonen, and J. B. Ketterson, "Strongly localized magnetization modes in permalloy antidot lattices," Applied Physics Letters **102**(15), 152412 (2013).
[5] M. P. Kostylev, A. A. Serga, T. Schneider, B. Leven, and B. Hillebrands, "Spin-wave logical gates," Applied Physics Letters **87**(15), 153501 (2005).
[6] T. Schneider, A. A. Serga, B. Leven, B. Hillebrands, R. L. Stamps, and M. P. Kostylev, "Realization of spin-wave logic gates," Applied Physics Letters **92**(2), 022505 (2008).
[7] B. Van de Wiele, A. Manzin, A. Vansteenkiste, O. Bottauscio, L. Dupre, and D. De Zutter, "A micromagnetic study of the reversal mechanism in permalloy antidot arrays," Journal of Applied Physics **111**(5), 053915 (2012).
[8] J. Ding, D. Tripathy, and A. O. Adeyeye, "Effect of antidot diameter on the dynamic response of nanoscale antidot arrays," Journal of Applied Physics **109**(07D304) (2011).
[9] J. Ding, D. Tripathy, and A. O. Adeyeye, "Dynamic response of antidot nanostructures with alternating hole diameters," EPL- Europhysics Letters **98**, 16004 (2012).
[10] R. L. Rodríguez-Suárez, J. L. Palma, E. O. Burgos, S. Michea, J. Escrig, J. C. Denardin, and C. Aliaga, "Ferromagnetic resonance investigation in permalloy magnetic antidot arrays on alumina nanoporous membranes," Journal of Magnetism and Magnetic Materials **350**, 88–93 (2014).
[11] Chengtao Yu, Michael J. Pechan, and Gary J. Mankey, "Dipolar induced, spatially localized resonance in magnetic antidot arrays," Applied Physics Letters **83**, 3948–3950 (2003).
[12] Stephan Martens, Ole Albrecht, Kornelius Nielsch, and Detlef Görlitz, "Local modes and two magnon scattering in ordered permalloy antidot arrays," Journal of Applied Physics **105**(07).
[13] V. Bhat, J. Woods, L. E. De Long, J. T. Hastings, V. V. Metlushko, K. Rivkin, O. Heinonen, J. Sklenar, and J. B. Ketterson, Broad-band FMR study of ferromagnetic thin films patterned with antidot lattices. **479**, 83–87 (2012).
[14] J Nogues and Ivan K Schuller, "Exchange bias," Journal of Magnetism and Magnetic Materials **192**, 203–232 (1999).
[15] R L Stamps, "Mechanisms for exchange bias," Journal of Physics D: Applied Physics **33**(23), R247–R268 (2000).
[16] A. O. Adeyeye, S. Goolaup, N. Singh, W. Jun, C. C. Wang, S. Jain, and D. Tripathy, "Reversal mechanisms in ferromagnetic nanostructures," IEEE Transactions on Magnetics **44**, 1935–1940 (2008).
[17] C C Wang, A O Adeyeye, and N Singh, "Magnetic antidot nanostructures: effect of lattice geometry," Nanotechnology **17**(6), 1629–1636 (2006).
[18] D. Tripathy, A. O. Adeyeye, and N. Singh, "Exchange bias in nanoscale antidot arrays," Applied Physics Letters **93**(2), 022502 (2008).
[19] D. Tripathy and A. O. Adeyeye, "Magnetization reversal in exchange biased antidot arrays," Journal of Applied Physics **105**(7), 07D703 (2009).
[20] M. Tofizur Rahman, Nazmun N. Shams, Ding Shuo Wang, and Chih-Huang Lai, "Enhanced exchange bias in sub-50-nm IrMn/CoFe nanostructure," Applied Physics Letters **94**(8), 082503 (2009).
[21] J. Nogués, J. Sort, V. Langlais, V. Skumryev, S. Suriñach, J. S. Muñoz, and M. D. Baró, "Exchange bias in nanostructures," Physics Reports **422**(3), 65–117 (2005).
[22] Wei Zhang, Dirk N. Weiss, and Kannan M. Krishnan, "Competing anisotropies and temperature dependence of exchange bias in CoIrMn metallic wire arrays fabricated by nanoimprint lithography," Journal of Applied Physics **107**(9), 09D724 (2010).
[23] J. Mohanty, S. Vandezande, S. Brems, M. J. Van Bael, T. Charlton, S. Langridge, R. M. Dalgliesh, K. Temst, and C. Van Haesendonck, "Magnetization reversal studies of continuous and patterned exchange biased nife/femn thin films," Applied Physics A **109**(1), 181–187 (2012).
[24] M. Kovylina, M. Erekhinsky, R. Morales, J. E. Villegas, I. K. Schuller, a. Labarta, and X. Batlle, "Tuning exchange bias in Ni/FeF 2 heterostructures using antidot arrays," Applied Physics Letters **95**(15), 152507 (2009).
[25] A. Hoffmann, M. Grimsditch, J. Pearson, J. Nogués, W. Macedo, and Ivan Schuller, "Tailoring the exchange bias via shape anisotropy in ferromagnetic/antiferromagnetic exchange-coupled systems," Physical Review B **67**(22), 220406 (2003).
[26] R. Morales, M. Kovylina, Ivan K. Schuller, a. Labarta, and X. Batlle, "Antiferromagnetic/ferromagnetic nanostructures for multidigit storage units," Applied Physics Letters **104**(3), 032401 (2014).

[27] R. Stamps, R. Camley, and R. Hicken, "Influence of exchange-coupled anisotropies on spin-wave frequencies in magnetic layered systems: Application to Co/CoO," Physical Review B **54**(6), 4159–4164 (1996).
[28] K.-W. Lin, M. Mirza, C. Shueh, H.-R. Huang, H.-F. Hsu, and J. Van Lierop, "Tailoring interfacial exchange coupling with low-energy ion beam bombardment: Tuning the interface roughness," Applied Physics Letters **100**(12), 122409 (2012).
[29] F. J. T. Goncalves, G. Paterson, S. O'Reilly, T. Drysdale, D. S. Schmool, and R. L. Stamps, Unpublished- modifying anisotropies in exchange biased and 2-d nano-structured systems, 2015.
[30] A. Vansteenkiste and B. Van De Wiele, "MUMAX: A new high-performance micromagnetic simulation tool," Journal of Magnetism and Magnetic Materials **323**, 2585–2591 (2011).